TO STUDY THERMAL PROPERTIES OF VARIOUS SOLIDS

BY

AURANGZEB

A Dissertation submitted in the partial fulfilment of the requirements of the degree of Master of Philosophy in Physics.

DEPARTMENT OF PHYSICS

QUAID-i-AZAM UNIVERSITY

ISLAMABAD

PAKISTAN

(1996)

CERTIFICATE

Certified that the experimental work in this dissertation was carried out and completed under my supervision.

(DR. ASGHARI MAQSOOD)
Supervisor

(DR. KAMALUDDIN AHMED)
Chairman
Department of Physics
Quaid-i-Azam University
ISLAMABAD

ACKNOWLEDGEMENTS

All praise to Almighty Allah, the most merciful and most compassionate, Who enabled me to complete this research successfully. I offer my humblest and sincerest words of thanks to His Holy Prophet Muhammad (peace be upon Him) who is a forever torch of guidance and knowledge for humanity.

I have really no words of thanks for my supervisor, Dr. Asghari Maqsood, whose sympathetic guidance, encouraging attitude and valuable discussions enabled me to complete my research work successfully. I cannot forget her polite and broadening behaviour which removed all difficulties in my way.

I am grateful to the Chairman, Department of Physics, Quaid-i-Azam University, Islamabad for providing all possible facilities for my research work and fruitful discussions in the accomplishment of this manuscript.

I am very thankful to the University Grants Commission, Pakistan for providing me financial support under the scheme, " Infaq Foundation Scholarships for Higher Studies".

I would like to acknowledge the valuable help rendered to me by my friends Mr. M. Saeed Malik, Mr. Iftikhar Ahmed, Mr. M. Maqsood, Mr. M. Saleem, Mr. Naseem Abbas Sherazi, Mr. M. Yousaf, Mr. Shahid Mahmood Ramay, Mr. Anis-ur-Rehman, Mr. Zahoor Ahmad, Mr. Shahid Rafique, Mr. Amjad Gilani, Mr. Mudassar Gilani, Mr. Majeed Anwer and Mr. Tahir Farid (my roommate).

I am also thankful to my aunt for her financial as well as moral support.

Finally, I also owe a debt of gratitude to my brothers and sisters who remembered me in their prayers for my success throughout the span of study.

(AURANGZEB)

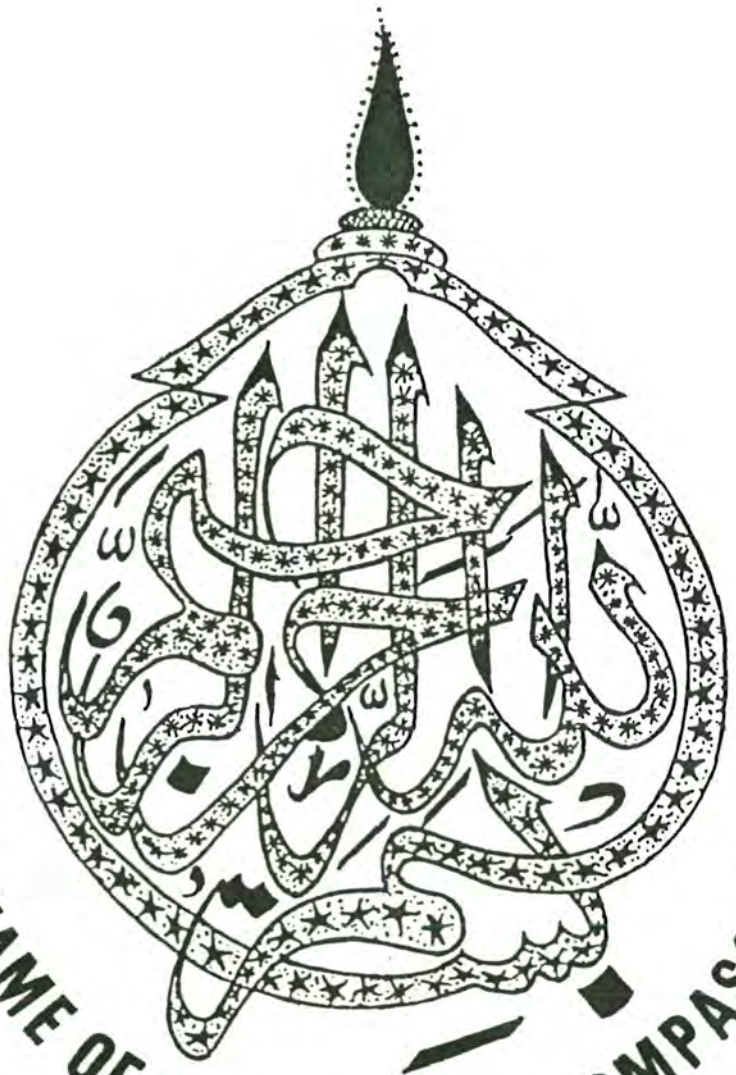

IN THE NAME OF ALLAH, THE COMPASSIONATE,
THE MERCIFUL.

264

" Science, like that nature to which it belongs, is neither limited by time nor space, it belongs to the world and is of no country and of no age".

_____ Humphry Devy

DEDICATED TO:

My (Late) parents,

Loving sisters

&

Brothers.

ABSTRACT

Thermal conductivity, thermal diffusivity and specific heat per unit volume of solids (rocks) at room temperature have been measured using Transient Plane Source (TPS) technique. The TPS-element is used both as a constant plane heat source and a sensor of temperature. The measurements were made on five samples, taken from north of Khewra town (at various positions from the base of sandstone). The variation of thermal conductivity as a function of position (from base) is reported. The porosity, chemical composition and x-ray diffraction of the samples as a function of position were determined. The effect of these parameters on thermal conductivity is also discussed.

CONTENTS

LIST OF FIGURES

LIST OF TABLES

LIST OF GRAPHS

CHAPTER 1

INTRODUCTION

According to the measured values of thermal conductivities of materials, all materials can be divided into two groups; first group consists of materials having high values of thermal conductivity (>10W/mK) and are known as good conductors, while second group consists of materials having low values of thermal conductivity and so named as insulators. Metals lie in the first group, which turn out to be good conductors of electricity also, whereas non-metals, powders and metal oxides belong to the second group.

It is our daily experience that when we heat one end of a solid material the other end also gets hot. This always happens when the two ends are at different temperatures. This is due to heat conduction through the solid, a process in which heat passes through the substance or the body itself. In a solid heat conduction takes place due to electrons flow, lattice vibrations and phonons.

Metals are not only good conductors of electricity but also of heat. This is because of an abundance of free electrons which act as current carriers as well as thermal energy carriers. The heat transfer depends upon the mean free path of the electrons which is very large or ideally infinite in the perfectly organized solids[1]. Therefore, the solids have very large value of conductivity. But in real materials, due to the presence of impurities and imperfections, this mean free path of the electrons between scattering decreases and so in turn the conductivity decreases.

In insulators, there are virtually no free electrons and the partnership between electrical and thermal conductivities no longer exists. It is interesting that thermal conductivity of an insulator is less than that of a metal by two or three orders of magnitude only. Therefore, we have good electrical insulator but no good heat insulators.

The process of conduction in the solid insulators is by the vibrations of the atoms or lattices themselves. When a part of a solid is heated, the atoms are set moving back and forth. The neighbouring atoms are nudged and in turn transfer their energy to the neighbours. This shows up on the macroscopic scale as flow of heat.

Like light photons, phonons are also quantized. Hence phonons are carriers of heat in non-metallic solids. The phonons can have infinite mean free path in the prefect crystals. But in real crystalline materials, they are scattered by phonons, crystal defects and impurities etc., and these imperfections are the cause of thermal resistance (resistance to heat flow).The inverse of the thermal resistance is the thermal conductance.

At high temperature phonon-phonon scattering appears due to the abundance of phonons. This leads to small mean free path of the phonons and the thermal conductivity becomes almost independent of the temperature of the body.

As the temperature decreases the mean free path increases and near a few degrees Kelvin the phonon-phonon scattering almost disappears and thermal conductivity of the insulator crystals is competitive to that for the metals. Thermal conductivity at low temperature falls as T^3 being limited by the sample size and the low density of the phonons[1].

The dominant thermal energy carriers in metals are free electrons and these belong to whole solid while in insulators, phonons are dominant thermal energy carriers and these belong to the whole crystal.

We know that, in electrical circuit, potential difference across parallel resistances is same and vice versa. We use this analogy for thermal conduction. Therefore for any solid the total thermal conductivity "λ_t", can be expressed as the sum of electronic conductivity "λ_e" due to free electron and lattice conductivity "λ_p" due to phonons . We write:

$$\lambda_t = \lambda_e + \lambda_p .$$

Where symbols used in the Fig. 1.1, mean:

R_e - Total resistance to electrons flow in a substance .

R_{el} - Resistance to electrons due to lattices.

R_{ed} - Resistance to electrons due to dislocations.

R_{ep} - Resistance to electrons due to point defects.

R_p - Total resistance to phonons flow in a substance .

R_{pl} - Resistance to phonons due to lattices.

R_{pd} - Resistance to phonons due to dislocations.

R_{pp} - Resistance to phonons due to point defects.

Q - Total heat into the substance.

κ_t - Total diffusivity

κ_e - Diffusivity due to electrons.

κ_p - Diffusivity due to phonons.

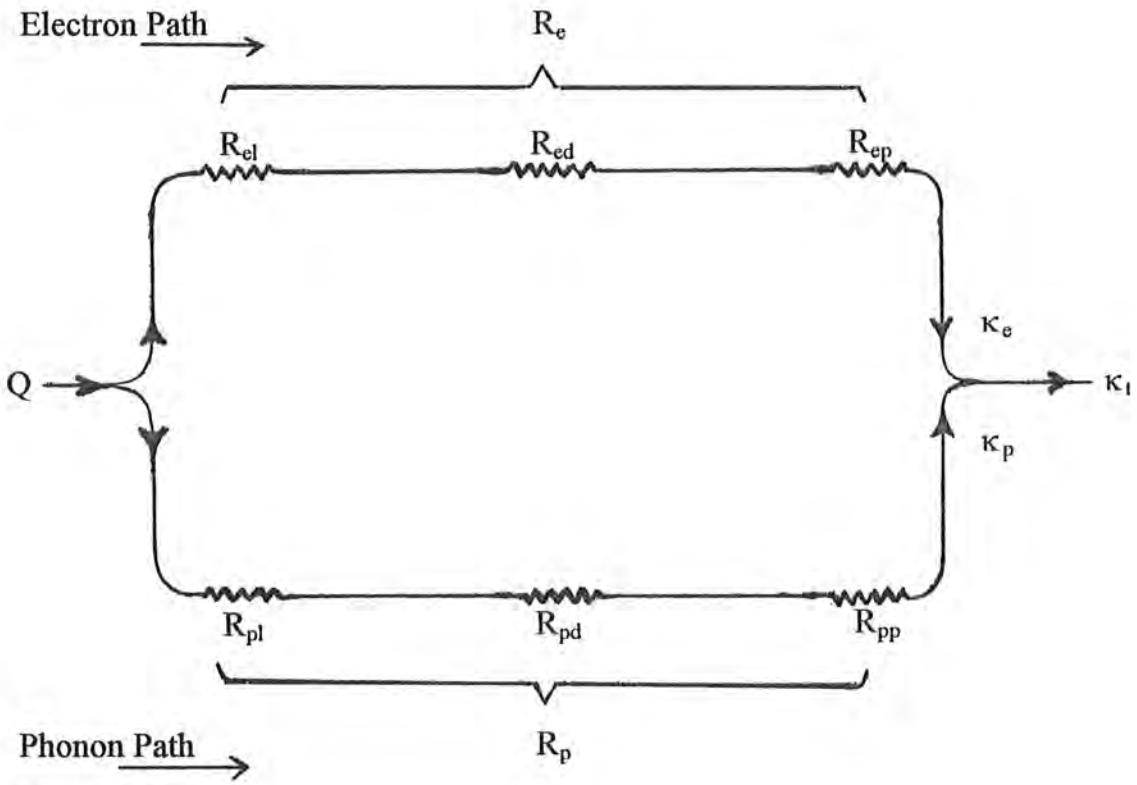

FIG. 1.1 ELECTRICAL ANALOG FOR THERMAL CONDUCTION.

CHAPTER 2

THERMAL CONDUCTIVITY AND EXPERIMENTAL METHODS FOR ITS DETERMINATION

2.1 Thermal conductivity

The thermal conductivity, λ, of a material is defined as the quantity of heat transmitted due to unit temperature gradient in unit time, under steady state conditions in a direction normal to the surface of unit area of cross-section.

The thermal diffusivity, κ, is defined by the relation:

$$\kappa = \lambda / \rho c_p ,$$

where ρ and c_p are the density and the heat capacity (at constant pressure) of the material. κ is thus the measurement of the ratio of heat transmission and energy storage capacity of the system[2].

In the case of isotropic medium the heat flux, $\vec{J}$, through unit area is given as:

$$\vec{J} = -\lambda(\vec{\nabla} T) \quad ,$$

where $\vec{\nabla} T$ is temperature gradient. Here $\vec{J}$ and $\vec{\nabla} T$ are collinear, but in case of

anisotropic medium $\vec{J}$ and $\vec{\nabla} T$ are not collinear, hence λ will be a tensor of nine components[3], given by:

$$J_i = -\sum_{i=1}^{3} \lambda_{ij} \frac{\partial T}{\partial x_i} ,$$

where only six components are different, for $\lambda_{ij}=\lambda_{ji}$. λ_{ij} is the ability of the material to transport heat in all directions (thermal conductivity). $\frac{\partial T}{\partial x_i}$ is the temperature gradient in i direction.

If we neglect the anisotropy with respect to heat conduction, as in case of polycrystalline and cubic crystals, then last equation can be written as:

$$\vec{J} = -\lambda(\vec{\nabla} T) . \qquad (2.1)$$

Consider an arbitrary volume V of a homogeneous isotropic solid within which no heat is being generated. If the temperature at any point (x,y,z) at time t is T(x,y,z) then the total flux of heat, or quantity of heat leaving a surface S enclosing volume V, per unit time is:

$$\oint_S d\vec{s}.(-\lambda\vec{\nabla} T).$$

Using Divergence theorem, we can change surface integral to volume integral as:

$$\oint_S d\vec{s}.(-\lambda\vec{\nabla} T) = \int_V \vec{\nabla}.(-\lambda\vec{\nabla T}). \qquad (2.2)$$

And the amount of heat entering the surface per unit time will be equal to:

$$\int_v \vec{\nabla}.(\lambda \vec{\nabla} T)dv.$$

If c_p is the specific heat of the solid at constant pressure and ρ is the mass density then heat contained in volume V is:

$$\int_v c_p \rho T dv,$$

and the increase in specific heat per unit time is:

$$\frac{\partial}{\partial t}\int_v c_p \rho T dv = \int_v c_p \rho \frac{\partial T}{\partial t} dv. \qquad (2.3)$$

Comparing eqs. (2.2) and (2.3), we get:

$$\int_v c_p \rho \frac{\partial T}{\partial t} dv = \int_v \vec{\nabla}.(\lambda \nabla \vec{T}) dv,$$

or

$$\int_v [c_p \rho \frac{\partial T}{\partial t} - \vec{\nabla}.(\lambda \nabla \vec{T}).] dv = 0.$$

Since volume V is arbitrary, the integrand in last equation is zero; resulting in the general equation of heat conduction:

$$\vec{\nabla}.(\lambda\vec{\nabla}T) = c_p\rho\frac{\partial T}{\partial t}.$$

If temperature variations are small and λ is almost independent of temperature, then:

$$\lambda\,\nabla^2 T = c_p\rho\frac{\partial T}{\partial t},$$

which may be written as:

$$\nabla^2 T = \frac{1}{\kappa}\frac{\partial T}{\partial t}. \qquad (2.4)$$

This is the basic equation of heat conduction for non-steady state or transient type measurement. But in steady state, $\frac{\partial T}{\partial t}$ reduces to zero and, therefore, the above equation reduces to Laplace equation:

$$\nabla^2 T = 0. \qquad (2.5)$$

There are numerous methods[4] for the determination of the thermal transport properties of the materials. Broadly, we can categorize them into two groups, namely Steady state methods and Non-steady state or Transient methods. Both these methods are based on the solutions of the eqs. (2.5) and (2.4) under

proper boundary conditions. Steady state methods make use of eq. (2.5), whereas non-steady state or transient methods use eq. (2.4).

The steady state methods require time consuming procedures to set up the experiment as well as to establish the steady state temperature gradient, especially in the case of insulating materials. Also, it is not possible to determine simultaneously the two thermal properties namely thermal conductivity and thermal diffusivity of the material using the steady state methods. To overcome these difficulties non steady state methods are utilized to measure the thermal transport properties.

Among these methods Transient Plane Source (TPS) technique is the best one, developed by S. E.Gustafasson [5]. The beauty of this method is that we can measure thermal conductivity and thermal diffusivity simultaneously. In this technique a plane source of heat, in the form of a spiral, is used. The source acts both as a source of heat and as a sensor of temperature increment of the sample. The TPS-sensor is made of nickel and is laminated with commercial plastic material (Kapton). The schematic diagram is shown in Fig. 2.1.

2.2 Theory of TPS-technique

The time dependent resistance of TPS-element during transient recording is given as:

$$R(t) = R_o\left(1+\alpha\overline{\Delta T(\tau)}\right), \qquad (2.6)$$

where R_o is the resistance of TPS-element before the initiation of transient recording, α is the temperature coefficient of resistivity and $\overline{\Delta T(\tau)}$ is the properly

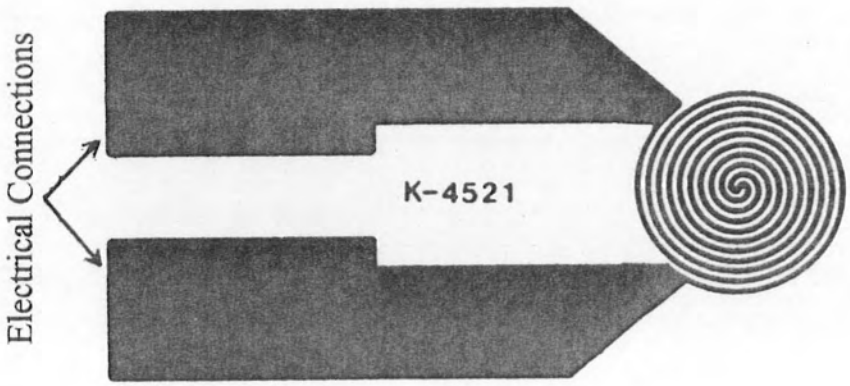

FIG. 2.1 SCHEMATIC DIAGRAM FOR TPS-ELEMENT.

calculated mean value of time dependent temperature increase of TPS-element.

The function τ is defined as:

$$\tau = (t/\theta)^{1/2} \quad , \quad \theta = a^2/\kappa, \tag{2.7}$$

where a is the radius of TPS element, κ is thermal diffusivity of the sample material under test and t is the time measured from the start of transient heating.

The probing depth[6] can be given as:

$$\Delta_p = \beta(\kappa t_{max})^{1/2}, \tag{2.8}$$

where t_{max} is the total time of transient recording and β is a constant of the order of unity.

To solve the thermal conductivity equation for non- steady state conditions we assume that TPS-element is located in yz-plane and inside an infinite solid with thermal conductivity λ, thermal diffusivity κ and heat capacity per unit volume ρc. If the heat is being generated at point (x', y', z', t'), we can write[7] the temperature increase at a point (x, y, z, t) due to an output power Q per unit area as:

$$\Delta T(y,z,t) = \left(8\pi^{3/2}\rho c_p\right)^{-1} \int_0^t dt'[k(t-t')]^{-3/2} \int_A dy'dz'Q(y',z',t') \times \exp\left[-\left\{(y-y')^2 + (z-z')^2\right\}/4\kappa(t-t')\right] \tag{2.9}$$

where A is the total area of the conducting pattern.

Substituting:

$$\sigma^2 = \frac{\kappa(t-t')}{a^2} \text{ we get:}$$

$$\Delta T(y,z,\tau) = \left(4\pi^{3/2}a\lambda\right)^{-1} \int_0^{\tau} d\sigma\sigma^{-2} \int_A dy'dz' Q\left(y',z',t-a^2\sigma^2/\kappa\right) \times \exp\left[-\left\{(y-y')^2+(z-z')^2\right\}/4a^2\sigma^2\right] \quad (2.10)$$

where $\tau = (t/\theta)^{1/2}$ and $\lambda = \kappa c_p \rho$.

If the plane source is in the form of a hot square of side 2a then eq. (2.10) can be written as:

$$\Delta T(y,z,\tau) = \left(4\pi^{3/2}a\lambda\right)^{-1} \int_0^{\tau} d\sigma\sigma^{-2} \int_{-a}^{+a} dy'dz' Q\left(y',z',t-a^2\sigma^2/\kappa\right) \times \exp\left[-\left\{(y-y')^2+(z-z')^2\right\}/4a^2\sigma^2\right] \quad (2.11)$$

Putting $\frac{(y-y')^2}{4a^2\sigma^2} = \eta^2$ and $\frac{(z-z')^2}{4a^2\sigma^2} = u^2$, eq. (2.11) becomes:

$$\Delta T(y,z,\tau) = (4\pi^{1/2}\lambda)^{-1} a \int_0^{\infty} d\sigma Q(y - 2a\sigma\eta, z - 2\sigma u, t - a^2\sigma^2/\kappa) \times \left[\operatorname{erf}\left(\frac{y+a}{2a\sigma}\right) - \operatorname{erf}\left(\frac{y-a}{2a\sigma}\right)\right]\left[\operatorname{erf}\left(\frac{z+a}{2a\sigma}\right) - \operatorname{erf}\left(\frac{z-a}{2a\sigma}\right)\right] \quad (2.12)$$

where

$$\frac{\sqrt{\pi}}{2}\operatorname{erf}(x) = \int_0^x \exp(-\zeta^2)d\zeta. \quad (2.13)$$

For the hot square the output constant power can be proved to be:

$$Q = \frac{P_o}{4a^2}.$$

So eq. (2.12) becomes:

$$\Delta T(y,z,\tau) = \frac{P_o}{16a\lambda\pi^{1/2}} \int_0^{\infty} d\sigma \left[\operatorname{erf}\left(\frac{y+a}{2a\sigma}\right) - \operatorname{erf}\left(\frac{y-a}{2a\sigma}\right)\right]\left[\operatorname{erf}\left(\frac{z+a}{2a\sigma}\right) - \operatorname{erf}\left(\frac{z-a}{2a\sigma}\right)\right]. \quad (2.14)$$

The mean temperature change over the area of the square can be written as:

$$\overline{\Delta T(\tau)} = \frac{1}{4a^2} \int_{-a}^{+a} dydz\Delta T(y,z,\tau). \quad (2.15)$$

Using eqs. (2.13) and (2.14), we get:

$$\overline{\Delta T(\tau)} = \frac{P_o}{4a^2.16a\pi\lambda^{1/2}} \int_0^{\infty} \int_{-a}^{+a} \left[\left\{ \operatorname{erf}\left(\frac{y+a}{2a\sigma}\right) - \operatorname{erf}\left(\frac{y-a}{2a\sigma}\right) \right\} \left\{ \operatorname{erf}\left(\frac{z+a}{2a\sigma}\right) - \operatorname{erf}\left(\frac{z-a}{2a\sigma}\right) \right\} \right] d\sigma dy dz. \tag{2.16}$$

To integrate over y we put:

$$\frac{y+a}{2a\sigma} = x \quad \text{and} \quad \frac{y-a}{2a\sigma} = x',$$

and get:

$$\int_{-a}^{+a} dy \left\{ \operatorname{erf}\left(\frac{y+a}{2a\sigma}\right) - \operatorname{erf}\left(\frac{y-a}{2a\sigma}\right) \right\} = 4a \left\{ \operatorname{erf}\left(\frac{1}{\sigma}\right) + \frac{\sigma}{\sqrt{\pi}} \exp\left(-\frac{1}{\sigma^2}\right) - \frac{\sigma}{\sqrt{\pi}} \right\}. \tag{2.17}$$

Similarly

$$\int_{-a}^{+a} dz \left\{ \operatorname{erf}\left(\frac{z+a}{2a\sigma}\right) - \operatorname{erf}\left(\frac{z-a}{2a\sigma}\right) \right\} = 4a \left\{ \operatorname{erf}\left(\frac{1}{\sigma}\right) + \frac{\sigma}{\sqrt{\pi}} \exp\left(-\frac{1}{\sigma^2}\right) - \frac{\sigma}{\sqrt{\pi}} \right\}. \tag{2.18}$$

Using eq.(2.17) and eq.(2.18) , we have:

$$\overline{\Delta T(\tau)} = \frac{P_o}{4a\lambda\pi^{1/2}} H(\tau), \tag{2.19}$$

where

$$H(\tau) = \int_0^{\infty} \left[.\operatorname{erf}\left(\frac{1}{\sigma}\right) + \frac{\sigma}{\sqrt{\pi}} \exp\left(-\frac{1}{\sigma^2}\right) - \frac{\sigma}{\sqrt{\pi}} \right]^2 d\sigma. \tag{2.20}$$

Due to this change in average temperature of the sensor the potential difference across it changes for a constant current passing through it. The voltage resolution for the measurement of this change in potential difference across the TPS-sensor is done with the help of a bridge circuit as shown in Fig. 2.2.

The power to the bridge circuit comes from a constant voltage power supply giving a constant input voltage V_{in}. To achieve a constant current in the circuit, resistance R_p in series to the source is used whose value is about 100 times the effective resistance of the bridge circuit. R_2 is adjustable resistance, R_s is the standard resistance and DVM is the digital voltmeter. The bridge is first operated in the balanced condition by making V_{in} small enough so that a small current flows through the non-linear resistance R_o which is the initial resistance of TPS-sensor before passing any current such that the temperature increment in R_o is negligible. Then R_2 is adjusted such that the potential difference across a and b is zero. Under this situation we get the condition :

$$\frac{R_1}{R_s} = \frac{R_2}{R_o} = \gamma .$$

The bridge is then switched over to the unbalanced mode with V_{in} such that a large enough current flows through R_o (resistance of the TPS-sensor) so as to give a temperature increment of about 1K. With this V_{in} voltage across the bridge, we get:

$$(I_1 - \Delta I_1)(R_s + \Delta R + R_o) = (I_2 + \Delta I_2)(R_1 + R_2). \qquad (2.21)$$

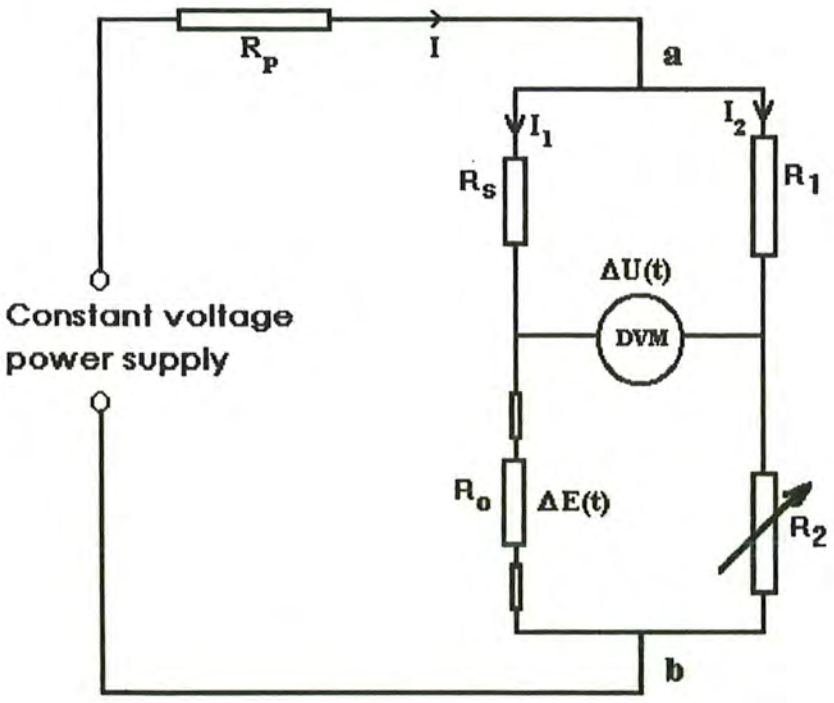

FIG.2.2 ELECTRICAL CIRCUIT DIAGRAM FOR TPS-TECHNIQUE.

Using

$$I_1(R_s + R_o) = I_2(R_1 + R_2),$$

and assuming $\Delta I_1 \Delta R \approx 0$, we get:

$$I_1(R_s + R_o) + I_1\Delta R - \Delta I_1(R_s + R_o) = I_2(R_1 + R_2) + \Delta I_2(R_1 + R_2),$$

$$I_1\Delta R - \Delta I_1(R_s + R_o) = \Delta I_2(R_1 + R_2). \qquad (2.22)$$

V_{in} can be written as:

$$V_{in} = R_p(I_1 + I_2 - \Delta I_1 + \Delta I_2) + (I_2 + \Delta I_2)(R_1 + R_2). \qquad (2.23)$$

As V_{in} is constant, therefore:

$$-R_p(\Delta I_1 - \Delta I_2) + \Delta I_2(R_1 + R_2) = 0,$$

$$\Delta I_2(R_1 + R_2 + R_p) = \Delta I_1 R_p,$$

$$\Delta I_2 = \frac{\Delta I_1 R_p}{(R_1 + R_2 + R_p)}. \qquad (2.24)$$

Substituting this in equation (2.22), we get:

$$I_1\Delta R - \Delta I_1\left(R_s + R_o\right) = \frac{\Delta I_1 R_p}{\left(R_1 + R_2 + R_p\right)}\left(R_1 + R_2\right),$$

$$I_1\Delta R = \Delta I_1\left(R_s + R_o\right) + \frac{\Delta I_1 R_p}{\left(R_1 + R_2 + R_p\right)}\left(R_1 + R_2\right),$$

$$I_1\Delta R = \Delta I_1\left[R_s + R_o + \frac{R_p\left(R_1 + R_2\right)}{\left(R_1 + R_2 + R_p\right)}\right],$$

$$\Delta I_1 = \frac{I_1\Delta R}{R_s + R_o + \dfrac{R_p\left(R_1 + R_2\right)}{\left(R_1 + R_2 + R_p\right)}}. \qquad (2.25)$$

The potential difference across the terminals a and b (Fig. 2.2.) due to the change in resistance of TPS-element is given as:

$$\Delta U = \left(I_1 - \Delta I_1\right)\left(R_o + \Delta R\right) - \left(I_2 + \Delta I_2\right)R_2. \qquad (2.26)$$

Using equations (2.21), (2.23), (2.25) and (2.26) togather with the condition $\Delta I_1\Delta R \approx 0$, we get:

$$\Delta U = \frac{R_s}{\left(R_o + R_s\right)} I_1\Delta R,$$

or

$$\Delta U = \frac{R_s}{(R_o + R_s)} I_1 \alpha R_o \overline{\Delta T}. \tag{2.27}$$

For a constant current $I_1 = I_o$, and from eq. (2.19), we can write:

$$\Delta U(\tau) = \frac{R_s}{(R_o + R_s)} [\alpha I_o^3 R_o^2][\zeta a \lambda]^{-1} H(\tau), \tag{2.28}$$

where $\zeta = 4\sqrt{\pi}$ is the constant whose value depends upon the shape of TPS-element. Therefore, for a disk type TPS-element only a is replaced by mean radius of the spiral.

From Fig. 2.2, we can calculate the value of $\Delta E(\tau)$, and:

$$\Delta E(\tau) = \Delta U(\tau)[1 - C.\Delta U(\tau)]^{-1}, \tag{2.29}$$

where

$$C = \frac{R_s . I_o}{1 + \frac{\gamma R_p}{\gamma(R_o + R_s) + R_p}}. \tag{2.30}$$

2.3 Advantages of TPS-technique:

1. Both the thermal conductivity and thermal diffusivity can be found simultaneously. Specific heat per unit volume can also be found.

2. In this technique very simple electrical circuit (bridge circuit) is used.

3. TPS element can be used repeatedly due to its stability and reliability.

2.4 Disadvantages of TPS-Technique:

1. To make large sized samples of dimensions >3.0×3.0×2.0 cm^3 is not possible under all circumstances.

2. This technique can not be used for gases.

CHAPTER 3

EXPERIMENTAL SETUP WITH RESULTS AND DISCUSSION

3.1 The mega scopic description of the samples

The samples (stones) were collected from north of Khewra Town through Pakistan Museum of Natural History, Islamabad. The stones had been taken from various positions above the base of sandstone. The mega scopic description of each sample[8] is given below:

3.1.1 Kh-Khs 9/88

Silty Shale to Clay: Purple brown to dark brown, weathers same, medium hard to soft, fine grained, poorly bedded, 90% clay, 10% silt and carbonates, gives strong effervescence with dilute HCl, poorly porous.

3.1.2 Kh-Khs 11/88

Fine Sandstone to Dolomitic Siltstone to Silty Dolomite: Light brown to greenish grey and grey, weathers to dark brown and greenish brown, medium hard to hard, fine grained, cross bedded, lenticular bedded, thinly laminated, 100% siltstone to fine sandstone in one part and in other part 60% siltstone to fine sandstone and 30% carbonates probably dolomite, 10% clay, gives strong effervescence with dilute HCl, poorly porous, porosity blocked due to clay and carbonate material.

3.1.3 Kh-Khs 15/88

Silty Sandy Calcareous Nodule: Whitish grey to brownish grey, weathers to dark brown, medium hard to hard, fine grained to finally crystalline crystals, lenticular bedded, cross bedded, 40% silty sand to sandy silt, 40% minerals, 20% silty clay, gives strong effervescence with dilute HCl, iron minerals may be expected.

3.1.4 Kh-Khs 22/88

Sandstone: Purple brown to dark brown, weathers to greyish brown, medium hard, fine grained, lenticular bedded, thinly bedded, cross bedded, 90% siltstone to fine sandstone, 10% silty clay, slightly calcareous, poor to fairly porous.

3.1.5 Kh-Khs 29/88

Sandstone: Yellowish brown to reddish brown, weathers to greyish white, medium hard, fine to medium grained, thinly laminated, lenticular bedded, cross bedded, 95% sandstone, 5% silty clay to silt, fairly porous.

3.2 Experimental setup and calibration measurements

3.2.1 Design of TPS-element

The measurements reported in this chapter were performed with TPS-element

of the type shown in Fig.2.1. This was made of 10 μm thick nickel foils with an insulation on each side of the metal pattern made of 30 μm thick Kapton.

No influence could be recorded from electrical connections which are shown in Fig. 2.1. These connecting leads have the same thickness as the metal pattern of the TPS-element. All TPS-elements had at room temperature a resistance of about 4 ohms[9] and a TCR (Temperature coefficient of resistivity) of around $4.6 \times 10^{-3} K^{-1}$.

3.2.2 Platinum resistance thermometer

To have an exact idea of temperature, a platinum wire resistance thermometer is used. The resistance variations in this thermometer were recorded by HP3478A type digital multimeter and respective temperature was noted from the standard calibration table for the thermometer. The calibration is often checked in our laboratory.

3.2.3 Temperature coefficient of resistivity (TCR)

Measurements of thermal transport properties were carried out by temperature variations in the test medium, and temperature dependence of resistance of the medium is given by eq. (2.6). In this equation α is the temperature coefficient of resistivity of the material, which is defined as, " The change in resistance of the material per unit resistance per degree rise in temperature". It is measured in K^{-1}. Also voltage changes are directly affected by TCR (α) as is obvious from eq. (2.27). So it is necessary to determine this coefficient precisely and accurately.

TCR can be calculated by using the formula:

$$\alpha = \frac{R_2 - R_1}{R_1(T_2 - T_1)}, \qquad (3.1)$$

where

R_1= Resistance of TPS-element at low temperature

R_2 = Resistance of TPS-element at high temperature

T_1 = Lower temperature of TPS-element

T_2 = Higher temperature of TPS-element.

Normally α was found to be 4.6×10^{-3} K^{-1}, at room temprature.

3.2.4 Sample preparation

The samples were cut in rectangular shape, having dimensions $6.0\times3.5\times2.0$ cm^3, with the cooperation of Department of Geophysics, Quaid-i-Azam university. Then the surfaces of the rectangular pieces were polished and made smooth. This is to ensure a good thermal contact between the sensor and the sample material, as the TPS-sensor is sandwiched between the two completely smooth slabs of the material in the sample holder. The change in voltage were recorded with a digital voltmeter which is online to a personal computer. The power input to the sample is adjusted according to the nature of the sample material[10] and corresponded in most cases between 0.06 - 0.16 W/cm^2.

3.3 Experimental procedure and calibration of the apparatus

The TPS-element is placed inside the sample halves and clamped to ensure good thermal contact. Prior to the start of measuring procedure the system is expected to be in equilibrium.

In experiments with insulating layers of such thickness it is necessary to delete voltage recordings during first few seconds because of the influence of insulating layers. Due to the size of heated area of TPS-element the characteristic time of experiment is so long that it is possible to delete a few seconds of recorded voltage values and still get very good results[10].

An important aspect of the design of any TPS-element is that the pattern should be such that as large part of the hot area as possible should be covered by the electrically conducting pattern, as long as there is good insulation between different parts of the pattern. This is directly related to the importance of minimizing the thermal contact resistance between the heated pattern and the surface(s) of the samples. It should be noted [10] that temperature difference across the insulating layer can, after a short initial transient, be considered constant.

An important point to be noted, while performing the experiment, was the time interval between two successive measurements on the same sample. It is observed that at room temperature this interval should be at least of three hours so that the sample may regain the equilibrium condition. If one keeps this time interval less than the stated value, the time voltage curve will not be of a steady form due to the existing non - equilibrium interactions.

Calibration measurement is essentially a comparison of any given quantity

with another quantity of the same kind chosen as a standard.The apparatus was calibrated with fused quartz sample.

Graph 1 gives the voltage versus time recording of an experiment. This plot indicates the time varying voltage across the sensor during the transient recording.

Graph 2 represents $\Delta U(\tau)$ against $H(\tau)$, which would be a straight line if θ has its proper value(chapter 2). It is possible to find this proper value of θ by repeating θ, because due to the size of the heated area of the TPS-element the characteristic time of the experiment is so long that it is possible to delete a few seconds of recorded voltage values as stated earlier. For this particular value of θ, we get thermal diffusivity from the relation (2.8).

Graph 3 shows the differential scattering of the experimental points. To get good results, this scattering should be uniformly distributed about the zero line. The value of thermal conductivity had been calculated for that value of τ for which the differential scattering of the experimental points is uniformly distributed about the zero line. This also depends upon the properly selected value of θ. Uniformly distributed data indicates the uniform flow of heat on both sides of the TPS-element.

3.4 Results and discussion

The experimental results of thermal conductivity, thermal diffusivity and specific heat per unit volume (at room temperature) for five samples, obtained by using TPS-technique,are shown in tables 1-5. Mean values of thermal conductivity, thermal diffusivity and specific heat per unit volume alongwith the standard deviations of the means (σ) in these results are also shown in these tables. Various

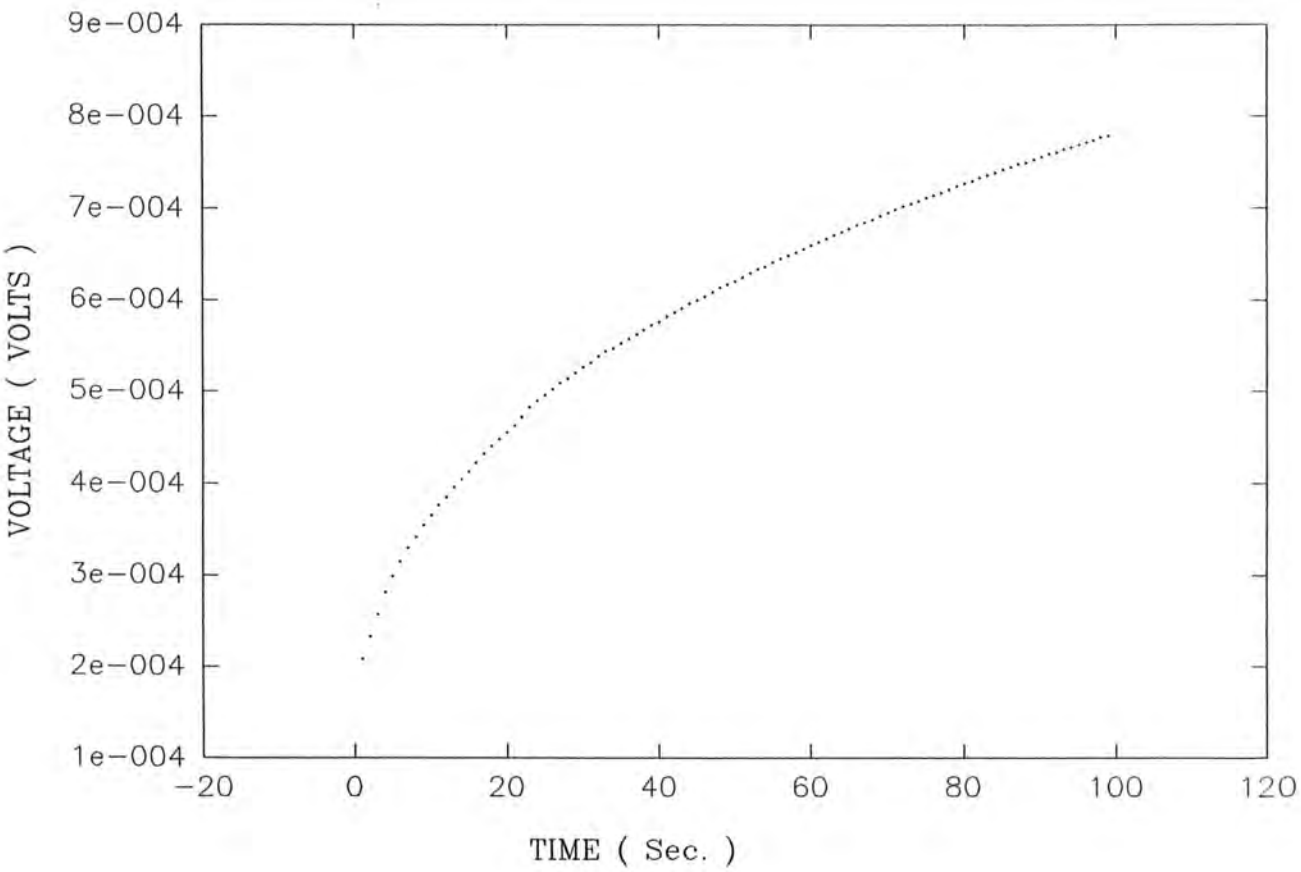

GRAPH: 1. VARIATION OF VOLTAGE WITH TIME

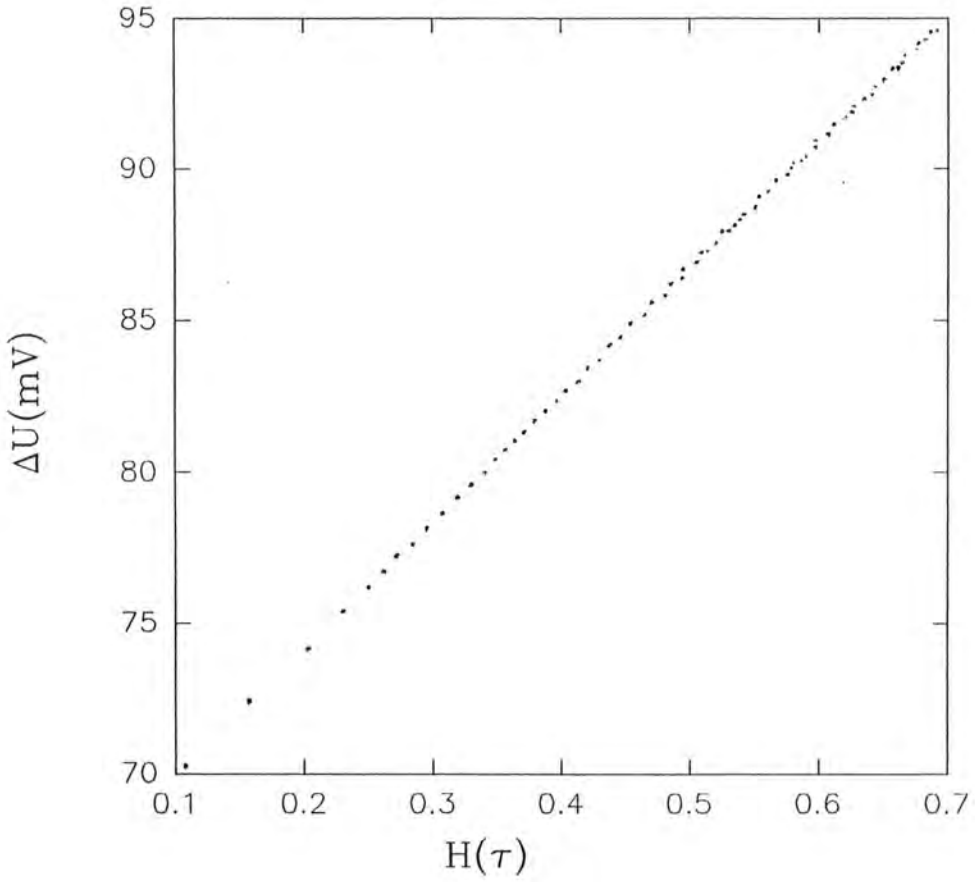

GRAPH: 2. REPRESENTATIVE PLOT OF H(τ) VERSUS ΔU(τ).

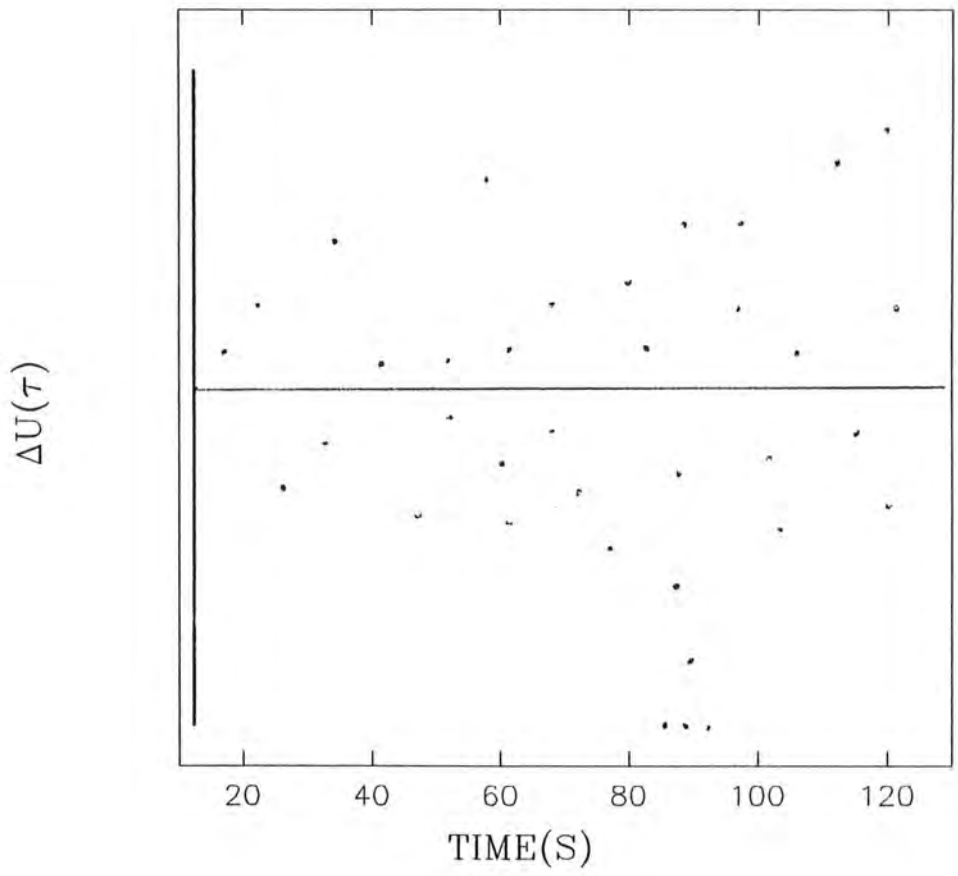

GRAPH: 3. REPRESENTATIVE DIFFERENTIAL SCATTERING DATA OF THE EXPERIMENTAL POINTS.

positions from the base of sandstone and corresponding values of thermal conductivities are plotted in graph 4. It can be noted from the tables that the values of the thermal conductivity in all the five samples of stones are ranging from 2.000 to 3.000W $m^{-1}K^{-1}$. This seems to be due to the basic nature and porosity of the individual samples. Thermal diffusivities of all the five samples are in the range of 0.800 to 2.500 mm^2/s, whereas the specific heat per unit volume ranges from 1.100 to 2.500 MJ m^{-3} K^{-1}.

3.4.1 Porosity

We know that porosity strongly affects the thermal conductivity of materials (greater the porosity, smaller the value of thermal conductivity) because in pores fluid is trapped which in turn blocks the convection process, so thermal conductivity decreases. One of the examples is the doubly ceiling buildings of the Quaid-i-Azam University.

A study of the individual samples indicates that most of the cementing materials are diagenetic and are responsible for blocking the porosity of the originally clean and porous sands. Table 6 provides the approximate percentage values of porosities of the samples[8]. This table indicates that the porosity ranges from 2-20%. Graph 5 is a plot of porosity versus position above the base of sandstone which is out of phase with the graph of thermal conductivity versus position (graph 4).

3.4.2 Chemical composition

In order to have better information about the thermal transport properties of

these stones, chemical composition of certain major elements; namely Ca, Fe, K, Mn, P, Si and Ti, was determined by the x-ray fluorescence technique. This information was provided by Nuclear Chemistry Division, Pinstech; Islamabad. Percentage chemical composition is given in table 7. From this table, we can see that it varies with position from the base of sandstone. These variations are shown in graphs 6-12.

3.4.3 X-ray diffraction studies

Most general method used for structure determination is X- ray diffraction. X-ray diffraction is an elastic scattering process in which a large number of atoms cooperate. Since the arrangement of the atoms in the lattice is periodic thus there must be some phase relationship of these atoms with the waves scattered by these atoms. According to optical diffraction theory constructive interference occurs if the phase difference or path difference between successive wave fronts is $n\lambda$, where n is an integer (1,2,3,....) and λ is wavelength of the incident x-rays. This holds according to Bragg's law:

$$n\lambda = 2d.\sin\theta, \qquad (3.1)$$

where d and θ are perpendicular distance between adjacent parallel planes and angle between the incident wave and refracted plane, respectively. Since, $\sin\theta$, can not exceed unity thus we may write the previous equation as:

$$\left[\frac{n\lambda}{2d}\right]\sin\theta < 1. \qquad (3.2)$$

Therefore $n\lambda$ must be less than 2d for diffraction. Smallest possible value of n is 1. Because n = 0 corresponds to the beam diffracted in same direction as transmitted beam and it can not be observed. Therefore condition for diffraction at any observable angle 2θ is $\lambda < 2d$ [1].

X-ray diffraction patterns of all the five samples were taken at the Dr. A. Q. Khan Research Laboratories. The patterns were taken using $CoK\alpha_1$ radiation ($\lambda = 1.789 \mathring{A}$). A comparison of the XRD patterns is shown in graph 13.

3.5 Conclusion

Since it is difficult to analyze the structure of stones (as for as the percentage composition of various compounds is concerned) by studying their x-ray diffraction pattern, their elementary analysis is made so that we are able to predict the percentage composition of constituents (compounds) of these elements and hence can compare their thermal conductivities to the conductivity of the sample.

Graphs 5-12 also give a comparison of thermal conductivity with porosity and percentage composition.

Let us consider only the range from 40m to 60m above the base of sandstone. In this range the value of thermal conductivity is comparatively high.

Graph 5 shows that the value of porosity is low for this range.

From graph 11 it is evident that the percentage composition of Si is large for this range; that is, amount of Quartz is also large. As thermal conductivity of Quartz is 1.4 $W\ m^{-1}K^{-1}$(at room temperature), therefore it has dominant effect on thermal conductivity of the samples.

Thermal conductivities [11] of Fe, Ca, K, Mn, P and Ti (at room temperature) are 804 $Wm^{-1}K^{-1}$, 201 $Wm^{-1}K^{-1}$, 102.5 $Wm^{-1}K^{-1}$, 78.1 $Wm^{-1}K^{-1}$, 2.36 $Wm^{-1}K^{-1}$ and 219 $Wm^{-1}K^{-1}$ respectively. As percentage composition of these elements is not so large as compared to the percentage composition of Si, their compounds will also be of small amount. Thus they do not play dominant role.

TABLE 1

Measurements of thermal conductivity, thermal diffusivity and heat capacity per unit volume of sample Kh-Khs 9/88, 26.40m above the base, using Kapton insulated TPS-element; at room temperature.

Exp. No.	Temp. K	Voltage Volts	Current mA	λ W m^{-1} K^{-1}	κ mm^2 sec^{-1}	ρc_p MJ m^{-3} K^{-1}
1.	303	10	172	3.162	1.884	1.678
2.	304	10	173	2.85	1.468	1.941
3.	304	10	173	2.889	1.424	2.029
4.	303	10	177	2.791	1.345	2.076
5.	301	10	175	3.035	1.615	1.879
6.	300	10	177	2.859	1.465	1.952
Mean value:				2.931	1.534	1.926
Standard Deviation:				0.127	0.176	

TABLE 2

Measurements of thermal conductivity, thermal diffusivity and heat capacity per unit volume of sample Kh-Khs 11/88, 45.92m above the base, using Kapton insulated TPS-element; at room temperature.

Exp. No.	Temp. K	Voltage Volts	Current mA	λ W m^{-1} K^{-1}	κ mm^2 sec^{-1}	ρc_p MJ m^{-3} K^{-1}
1.	300	10	173	2.587	1.337	1.935
2.	302	10	173	2.774	1.650	1.681
3.	303	10	177	2.726	1.558	1.750
4.	301	10	175	2.703	1.680	1.609
5.	300	10	168	2.683	2.077	1.292
6.	300	10	175	2.893	1.611	1.796
Mean value:				2.727	1.652	1.677
Standard Deviation:				0.093	0.220	

TABLE 3

Measurements of thermal conductivity, thermal diffusivity and heat capacity per unit volume of sample Kh- Khs 15/88, 54.25m above the base, using Kapton insulated TPS-element; at room temperature.

Exp. No.	Temp. K	Voltage Volts	Current mA	λ W m^{-1} K^{-1}	κ mm^2 sec^{-1}	ρc_p MJ m^{-3} K^{-1}
1.	306	12	210	2.856	1.607	1.777
2.	305	10	174	2.919	1.306	2.235
3.	304	10	172	3.196	1.648	1.940
4.	304	10	177	3.041	1.527	1.991
5.	303	10	177	3.044	1.316	2.312
6.	305	10	175	3.127	1.520	2.057
Mean value:				3.031	1.487	2.052
Standard Deviation:				0.115	0.132	

TABLE 4

Measurements of thermal conductivity, thermal diffusivity and heat capacity per unit volume of sample Kh-Khs 22/88, 26.40m above the base, using Kapton insulated TPS-element; at room temperature.

Exp. No.	Temp. K	Voltage Volts	Current mA	λ W m^{-1} K^{-1}	κ mm^2 sec^{-1}	ρc_p MJ m^{-3} K^{-1}
1.	300	10	175	2.569	1.261	2.037
2.	304	10	177	2.878	1.956	1.741
3.	303	10	177	2.769	1.705	1.624
4.	302	10	174	2.837	2.469	1.149
5.	301	10	175	2.682	1.321	2.030
6.	300	10	176	2.451	1.115	2.198
Mean value:				2.698	1.638	1.752
Standard Deviation:				0.150	0.468	

TABLE 5

Measurements of thermal conductivity, thermal diffusivity and heat capacity per unit volume of sample Kh-Khs 29/88, 26.40m above the base, using Kapton insulated TPS-element; at room temperature.

Exp. No.	Temp. K	Voltage Volts	Current mA	λ $W\ m^{-1}\ K^{-1}$	κ $mm^2\ sec^{-1}$	ρc_p $MJ\ m^{-3}\ K^{-1}$
1.	302	10	177	2.222	0.924	2.405
2.	301	10	175	2.333	1.036	2.252
3.	301	10	173	2.319	1.285	1.804
4.	301	10	175	2.037	0.979	2.080
5.	301	10	175	2.109	1.026	2.055
6.	301	10	175	2.095	0.899	2.330
Mean value:				2.186	1.025	2.154
Standard Deviation:				0.113	0.126	

TABLE 6

Measurement of percentage porosity

Sample no.	Position from base (m)	Porosity (%)
09/88	26.40	7*
11/88	45.92	6
15/88	54.25	2
22/88	74.73	15*
29/88	119.89	20

* means roughly calculated values (not available in literature).

TABLE 7

Concentration of constituents expressed in percentage unless specified

Sample no.	Position from base (m)	Ca	Fe	K	Mn*	P*	Si	Ti
09/88	26.40	4.07	1.62	4.28	587	488	25.64	0.29
11/88	45.92	1.77	2.24	4.63	453	761	27.75	0.65
15/88	54.25	3.04	1.35	3.32	337	303	30.11	0.24
22/88	74.73	2.91	1.32	2.35	356	187	35.92	0.12
29/88	119.89	4.40	0.86	2.06	602	<50	33.20	0.17

* means concentration in ppm (parts per million).

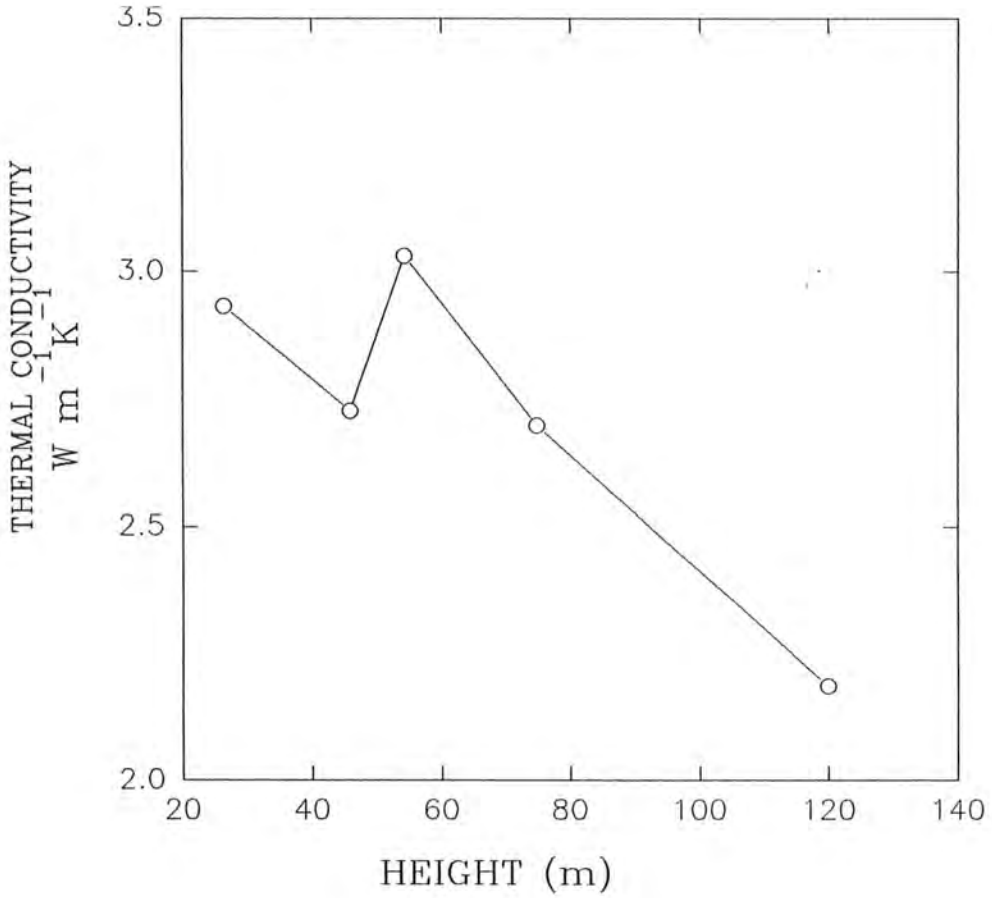

GRAPH: 4. VARIATION OF THERMAL CONDUCTIVITY WITH HEIGHT.

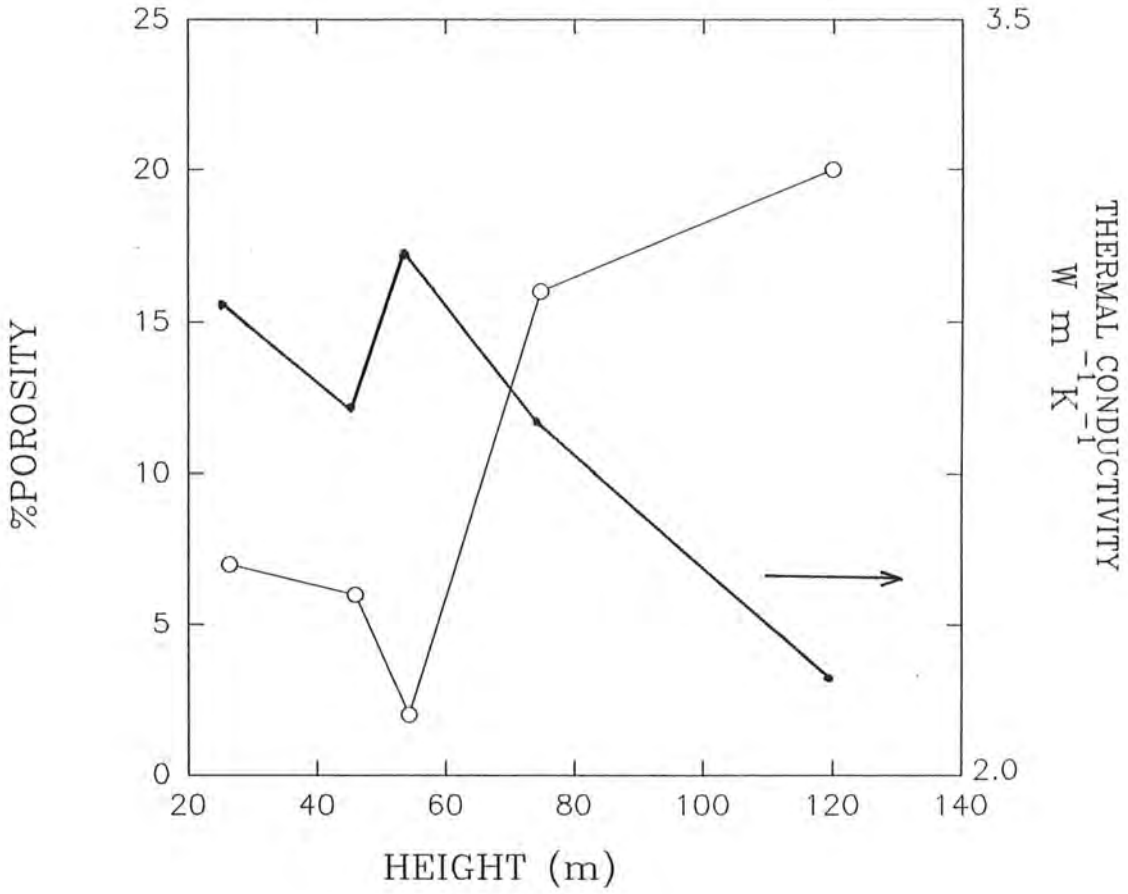

GRAPH: 5. VARIATION OF POROSITY WITH HEIGHT.

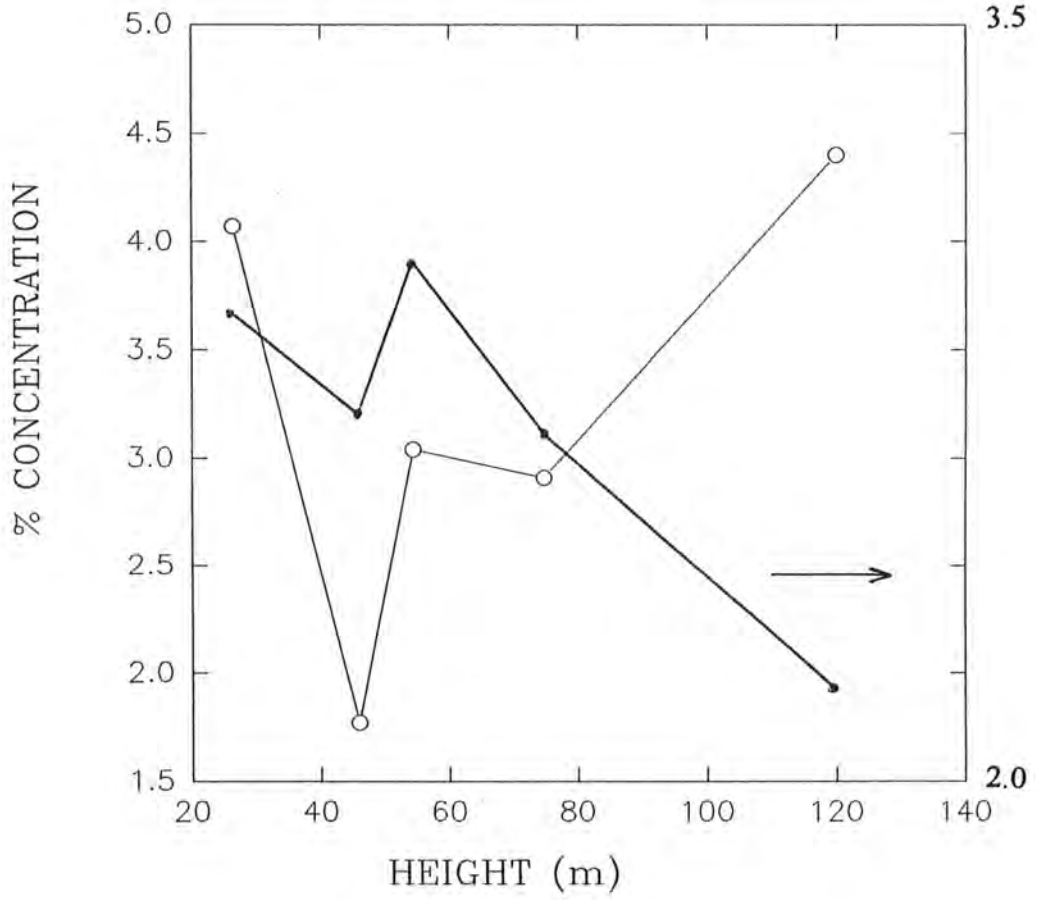

GRAPH 6. VARIATION OF PERCENTAGE CONCENTRATION OF Ca WITH HEIGHT.

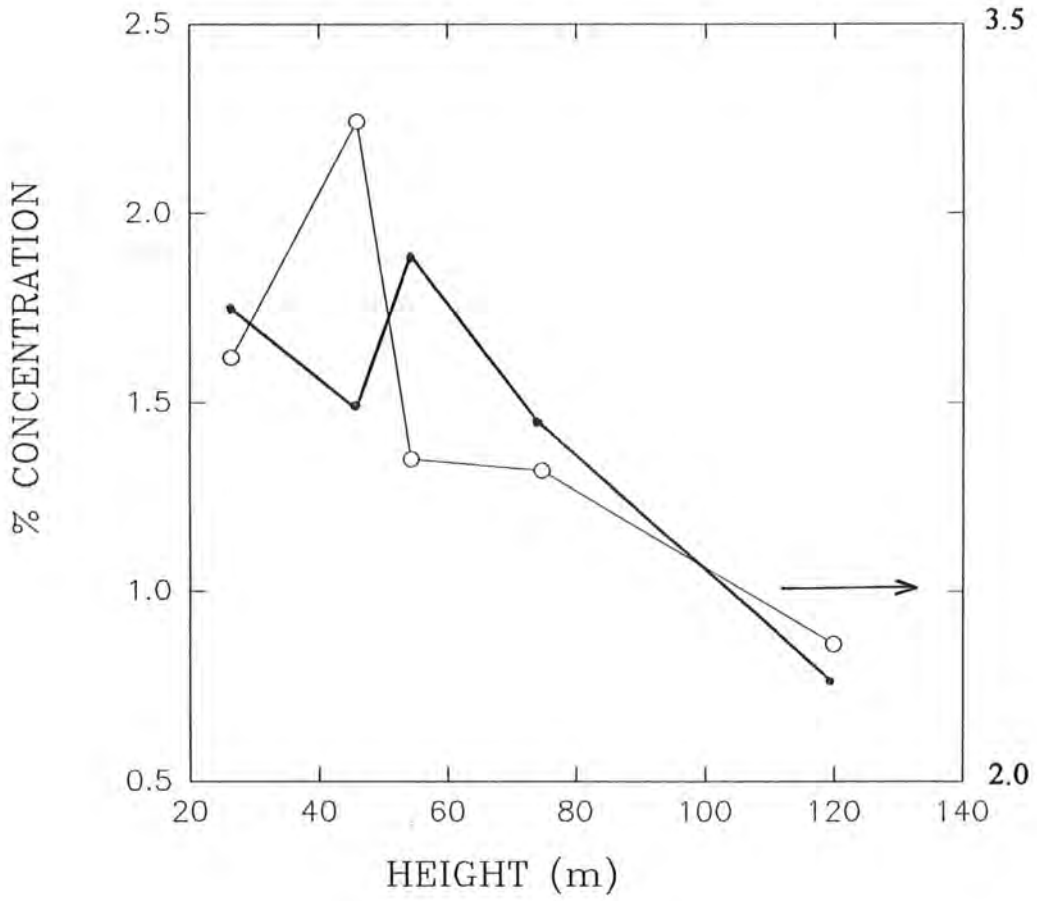

GRAPH 7. VARIATION OF PERCENTAGE CONCENTRATION OF Fe WITH HEIGHT.

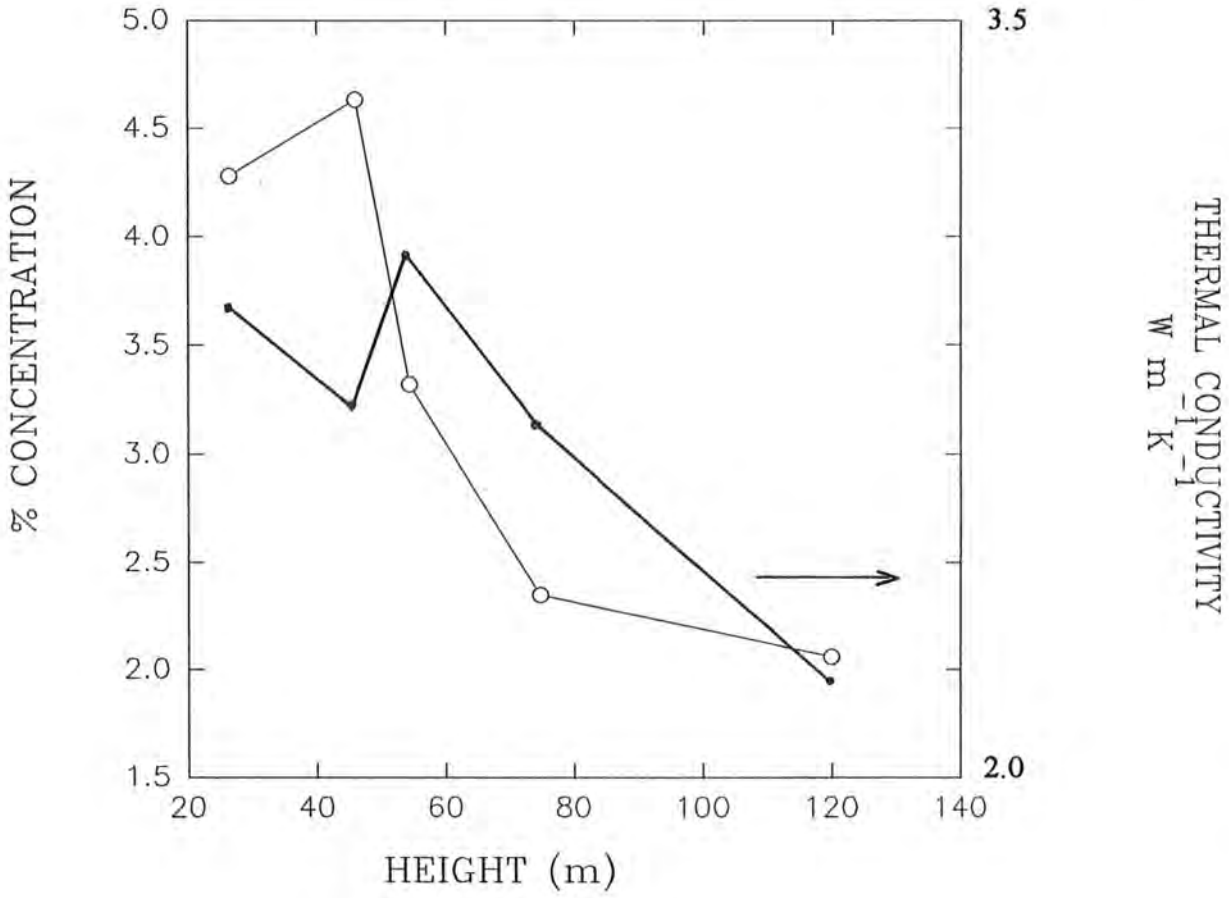

GRAPH 8. VARIATION OF PERCENTAGE CONCENTRATION OF K WITH HEIGHT.

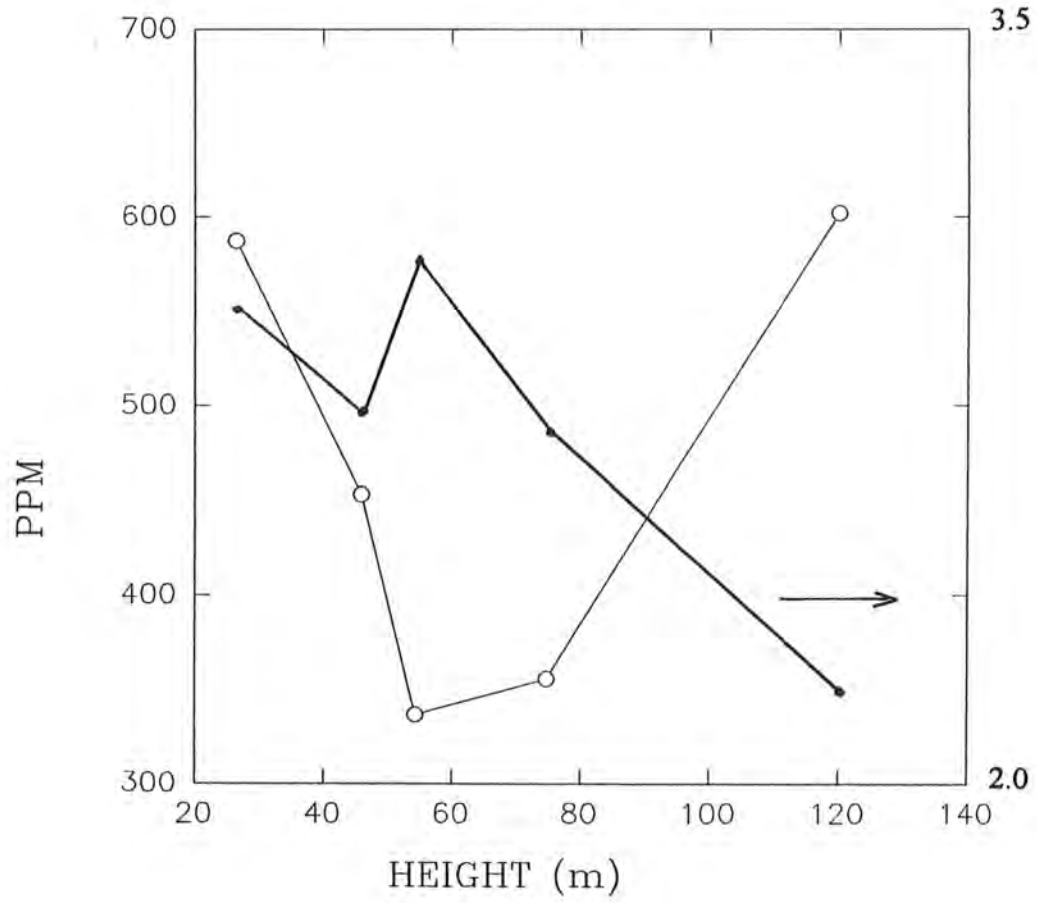

GRAPH 9. VARIATION OF PERCENTAGE CONCENTRATION OF Mn WITH HEIGHT.

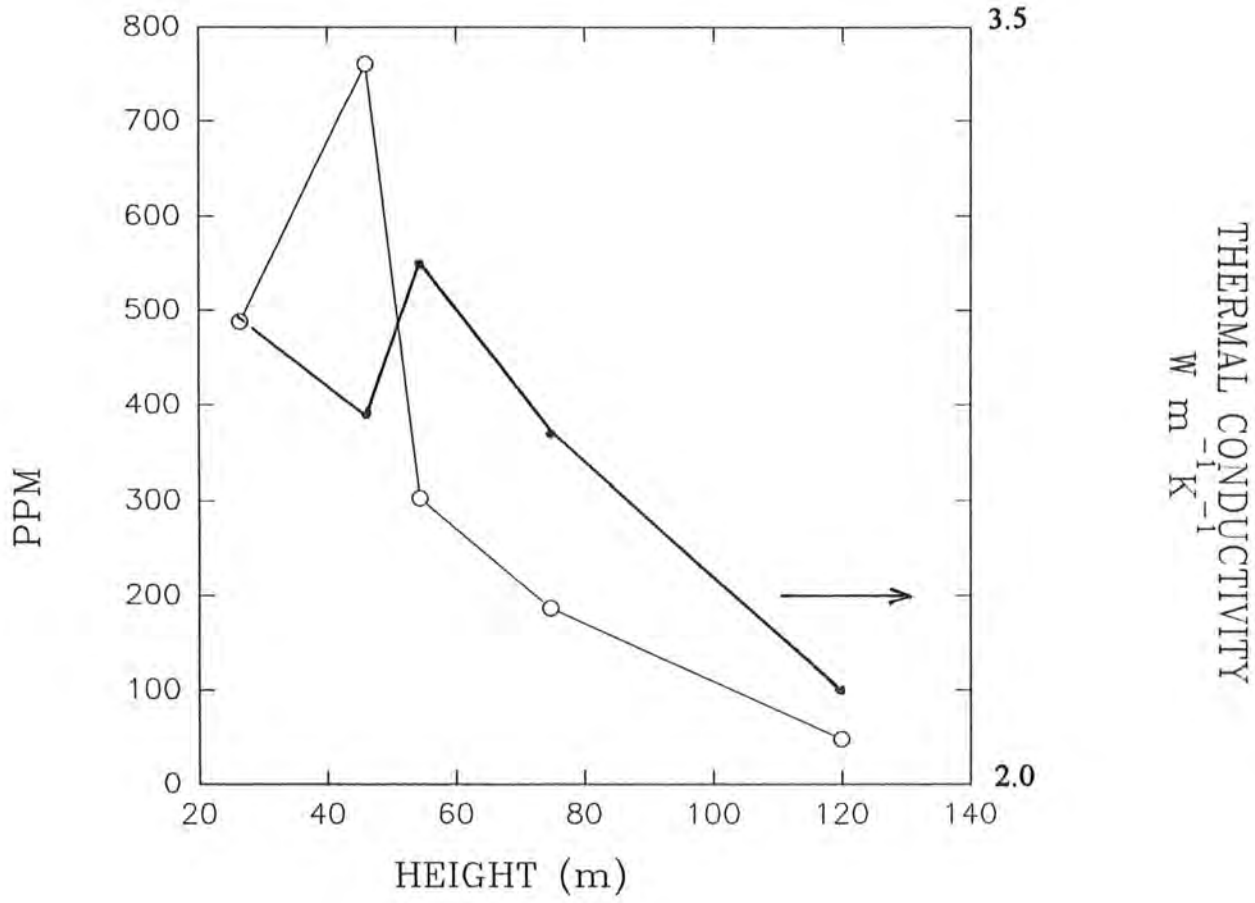

GRAPH 10. VARIATION OF PERCENTAGE CONCENTRATION OF P WITH HEIGHT.

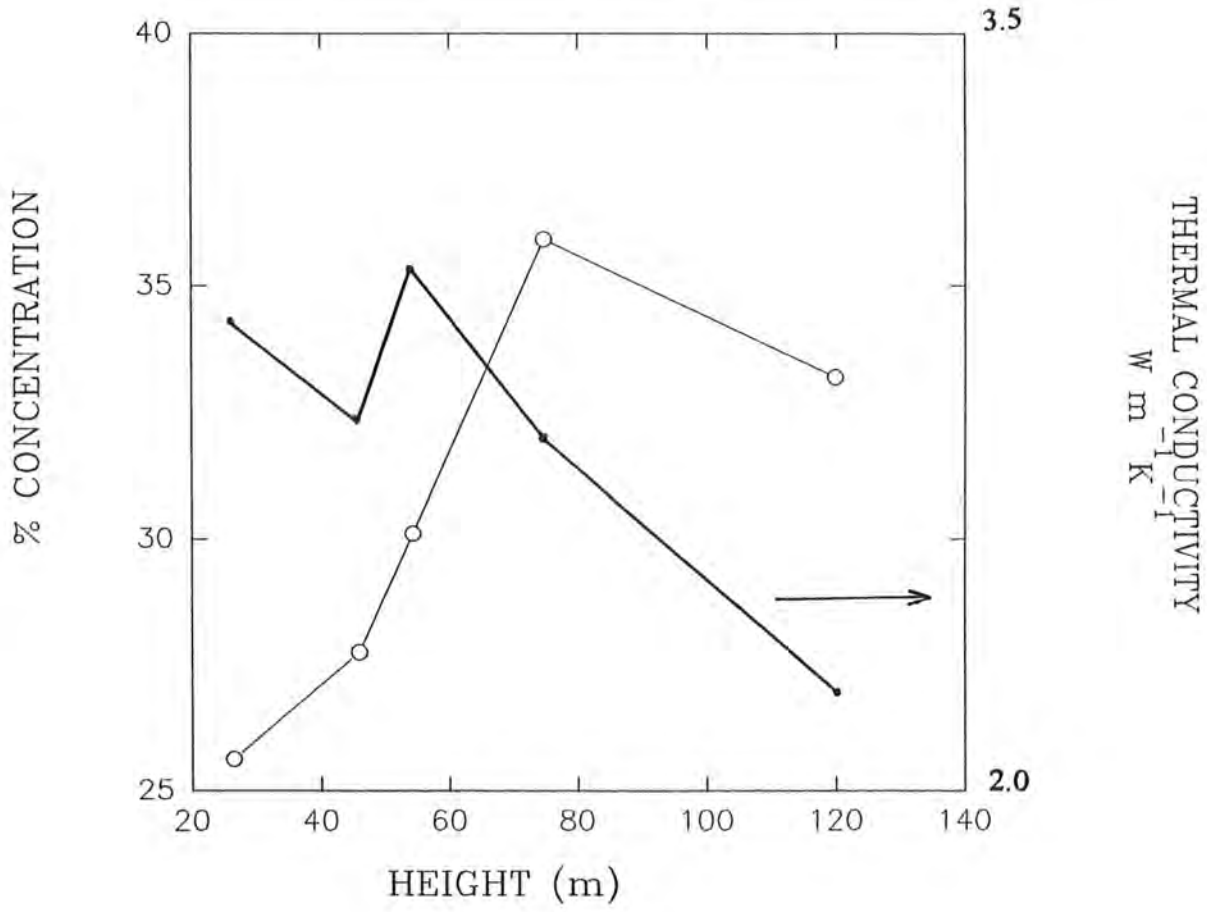

GRAPH: 11. VARIATION OF PERCENTAGE CONCENTRATION OF Si WITH HEIGHT.

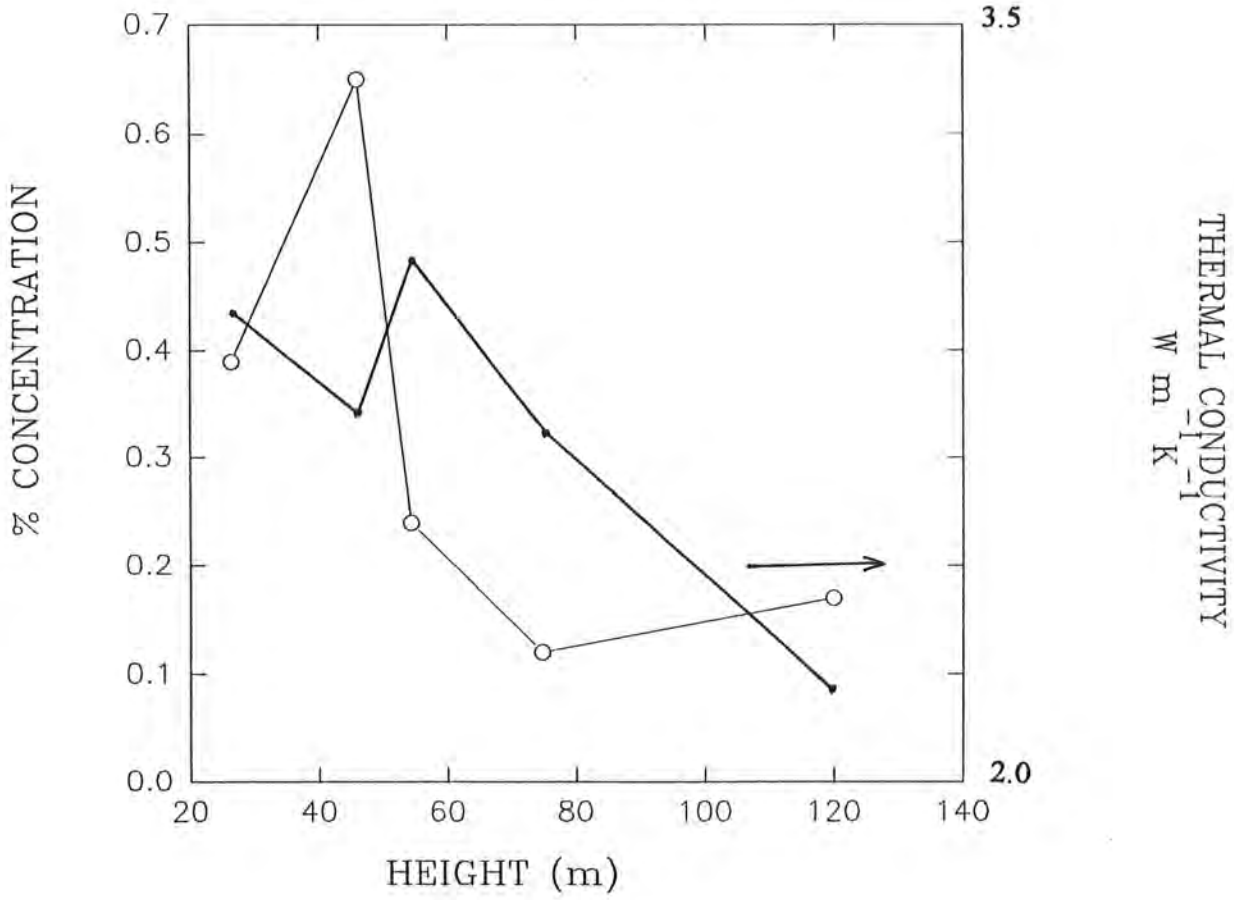

GRAPH 12. VARIATION OF PERCENTAGE CONCENTRATION OF Ti WITH HEIGHT.

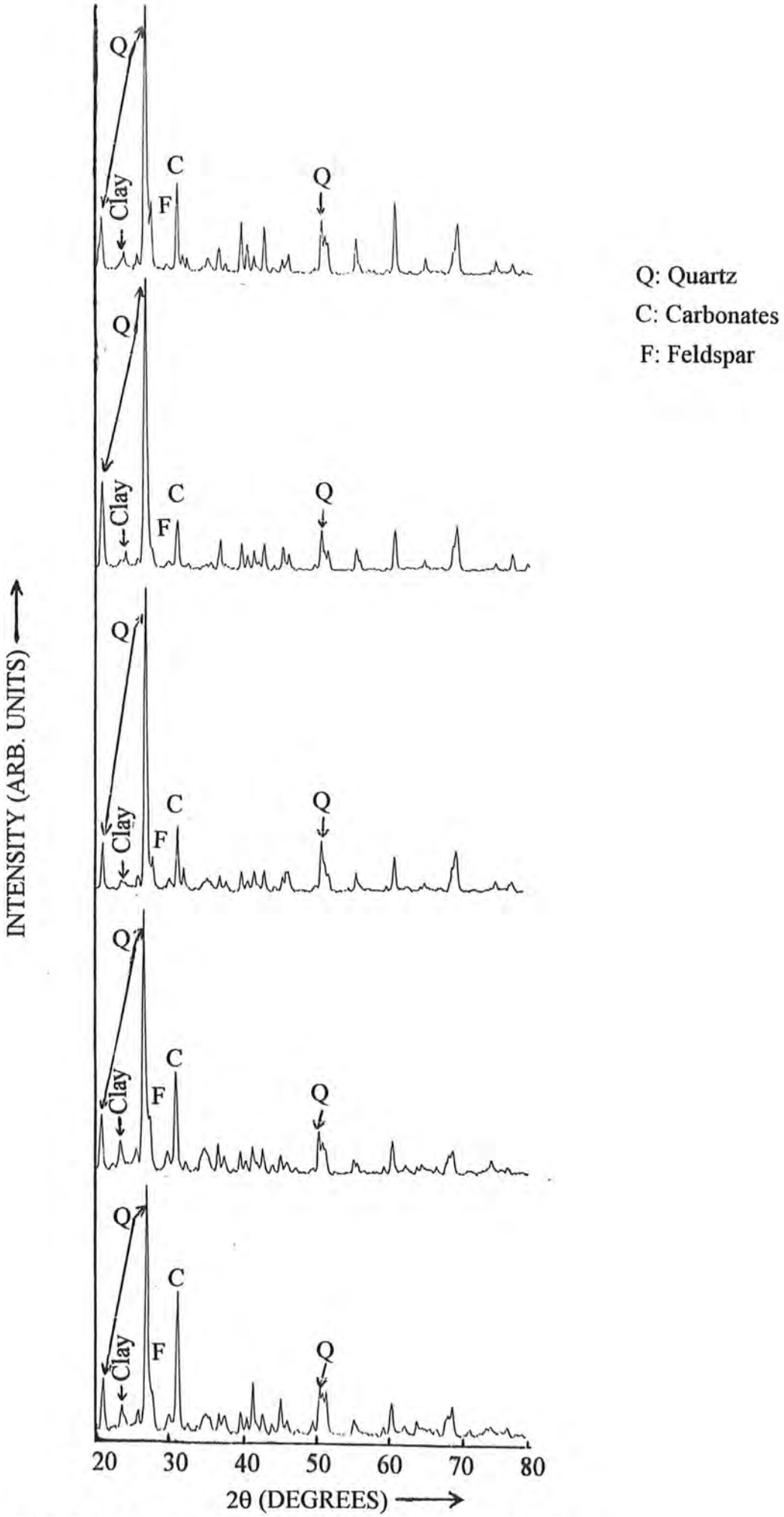

GRAPH: 13. COMPARISON OF XRD PATTERNS.

REFERENCES

1. Charles Kittel, "Introduction to Solid State Physics", 3rd. ed. (1966) 187, 165, 38.

2. M. N. Ozisik, "Heat Transfer a Basic Approach", McGraw Hills, New York, (1989) 23.

3. B. M. Suleiman: Ph. D. Thesis, Chalmer ' s University of Technology, Sweden (1994) 7.

4. M.A. Chohan: Ph.D. Thesis, Chalmer ' s University of Technology, Sweden, (1987).

5. S.E. Gustafsson: Rev. Sci. Instrum. 62, (1991) 797.

6. S.E. Gustafsson, M.A. Chohan, K. Ahmed and A. Maqsood: J. Appl. Phys. 55 (1984) 3348.

7. H. S. Carslaw and J. C. Jaeger, "Conduction of Heat in Solids", 2nd ed.,Oxford University Press (1959) 255.

8. Dr. S. R. H. Baqri, " Final Technical Report on Mineralogy and Geochemistry of the Cambrian Formations in Salt Range", Ist. ed. (1988)160,188.